Available online at www.sciencedirect.com

ScienceDirect

Procedia Materials Science 8 (2015) 108 – 116

Procedia Materials Science

www.elsevier.com/locate/procedia

International Congress of Science and Technology of Metallurgy and Materials, SAM - CONAMET 2013

Quantification of the Fracture Surface Profiles resulting from Different Loading Conditions on Ductile Irons

Diego Fernandino[(a)]*and Roberto Boeri[(a)]

[a]*División Metalurgia-INTEMA-CONICET-Universidad Nacional de Mar del Plata, Juan B Justo 4302, B7608FDQ, Mar del Plata, Argentina.*

Abstract

This study focuses on the characterization of the roughness of the fracture surfaces of spheroidal graphite irons of different matrix microstructures, generated under impact, bending and fatigue loading conditions. The fracture profiles were analyzed qualitatively by means of optical microscopy and quantitatively by means of the determination of the Rs and Ry topographic parameters. The values of Rs and Ry measured on the samples show changes as a result of changes in the matrix microstructure and the loading condition. Therefore, those values are potentially useful to identify the loading conditions that originated the fracture, and provide additional information to the classical fractographic analysis.

Selection and peer-review under responsibility of the scientific committee of SAM - CONAMET 2013

*Keywords:*Ductile iron; Fracture profile; Fracture surface; Impact, Bending; Fatigue

Nomenclature

L’	Projected length of the fracture profile
Lt	Actual length of the fracture profile
Rs	Superficial Roughness
Ry	Peak to valley ratio from the fracture profile
S_A	Projected fracture area
St	Actual fracture area

Selection and peer-review under responsibility of the scientific committee of SAM - CONAMET 2013
doi:10.1016/j.mspro.2015.04.054

1. Introduction

Ductile Irons (DI) are a family of cast irons that is increasingly applied in the construction of high stressed parts of machines and vehicles. As DI parts are frequently used in highly stressed parts, failure events take place, and it is essential to perform failure analysis to identify the causes of fracture and to provide corrective actions to guarantee safe operation. The fractographic study is a fundamental step in the failure analysis of a metallic part. The relationship between microstructural features of the material and the working conditions on the DI fracture processes have been analyzed in the literature, Rajnovic et.al (2008), Di Cocco et.al.(2010), Eldoky et.al.(1986), Iacoviello et. al.(2008), Greno et.al.(1999), Masud, et.al. (2003), Cavallini et.al. (2008), Chapetti et.al. (2000), Hafiz(2005), Shibutani et. al.(1999),Voigt.et. al. (1986), Jen et.al. (1992). In addition, the progress in modelling techniques, as reported by Bonora et.al (2005) and Ortiz et.al (2001),has allowed to validate some fracture mechanisms proposed by different authors. The fractographic characteristics identified for DI differ from the usual in steels and other metallic alloys. The presence of spheroidal graphite and the last to freeze zones (LTF), microsegregated and with presence of defects, have a strong influence on the morphology of the fracture surface. The role of the graphite nodules in the fracture processes was study by Liu et.al. (2002) and Dai et.al. (2001) although there is no general agreement among the authors. In most cases, given the inherent difficulty of experimentation involved, mechanisms that have not been yet verified have been proposed. Only few works have carried out a systematic analysis focused on the interpretation of the DI fracture surfaces generated by different load conditions and environments. In fact, the fractographic analyses reported in most works are secondary to a study of mechanical properties. Therefore, there is limited information available. This lack of information can be considered to be an obstacle for the application of these alloys since, for example, it is very difficult to extract information from a fractographic analysis and, therefore, to obtain information from one of the more important diagnosis elements. In this context, there is a need to study in detail the fractography of DI. In consequence, this work focuses on the study of the fracture surface of DI, specifying the analysis in the characterization of the fracture profiles resulting from several combinations of microstructures and mechanical solicitations.

2. Experimental procedure

2.1 Materials

One DI melt was prepared in a medium frequency induction furnace. Cu, Ni and Mn were added in order to provide sufficient austemperability, as was shown in the studies carried out by Voigy et.al (1991). The chemical compositions of the melts were determined by using a Baird DV6 spectrometer. One inch 'Y' blocks were cast in sand molds (ASTM A897M). The microconstituents as well as the nodule count, nodularity and nodule size were quantified by using an optical microscope OLYMPUS PMG3 and the Image-Pro Plus software (Media Cybernetics). A set of "Y" blocks were initially ferritized following an annealing heat treatment cycle in order to standardize the initial microstructure and to improve machinability. The heat treatment cycles carried out to obtain the five different microstructures are listed in Table 1.

Table 1. Heat treatment cycles

Microstructure	Heat treatment cycle
Pearlitic	As cast microstructure
Ferritic	Austenized for 4 hour at 900ºC, cooled down to 750º and held for 20 hours
Ausferritic (360)	Austenized for 1 hour at 900ºCand then austempered at 360º for 90 minutes
Ausferritic (280)	Austenized for 1 hour at 900ºCand then austempered at 280º for 90 minutes
Tempered Martensite	Austenized for 1 hour at 900ºC and quenched in water. Tempered for 1 hour at 250ºC

2.2 Mechanical Testing

Brinell hardness tests were carried out with a universal testing machine Ibertest, following the recommendations of the ASTM E10-01. The reported values are the average of at least three measurements.

V-notched Charpy impact specimens of 10x10x55 mm for impact and three point bending test (ASTM E23), and SEN(B) specimens of 10x20x90 mm for fatigue test (ASTM E399) were machined from Y blocks. The impact tests were performed by using a pendulum AMSLER 130/688, with a maximum energy of 300J, at four different test temperatures. Three-point bending tests were performed by using a universal testing machine Morh&Federhaff with a cross head displacement rate of $8.4x10^{-3}$ mm/sec. For the fatigue test, SEN(B) specimens were broken using a displacement controlled mechanical testing machine with a double eccentric actuator. A constant eccentricity of e = 0.145mm and R=0 was chosen for all tests. Stable crack propagation was attained following these conditions under small scale plasticity. The frequency of the cyclic load was of 25 Hz.

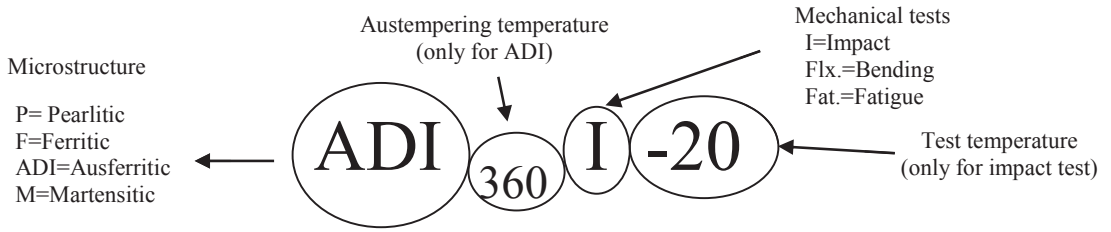

Fig. 1. Identification of the specimens.

2.3 Data processing and analysis

In order to obtain and analyze the fracture profiles of the samples tested, each fracture surface was cut along a perpendicular plane to the V-notch. The Underwood criterion was used to define the fracture surface roughness parameters, Underwood et.al (1987). For the numerical quantification of the surface roughness parameters, the Image-ProPlus software was used. The results obtained were the average of twenty fields of 529 by 397 μm (micrographs at 100x) in five successive layers in steps of 500 μm. A scheme of some parameters used is shown in Fig.2. Lt is the value of the actual length of the fracture profile whereas L' is the projected length of the fracture profile.

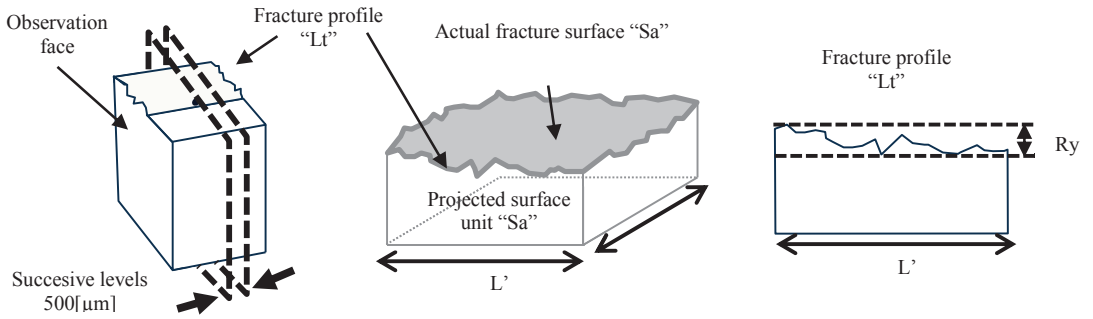

Fig.2. Schematic showing the definition of the topographic parameters measured on the fracture profiles.

Based on the measurements of Lt and L' on the fracture profiles, Rl and Rs values were calculated using Eqs. 1and 2, respectively. Rs was accounted for as the relation between the true fracture surface area (St) and the projected fracture surface area (S_A), that is, as measure of the superficial roughness (Eq.3). Moreover, the Ry value was obtained from the peak-valley ratio on the fracture profile (the difference between the height of the highest peak

and the height of the deepest valley). As the number of measurements of a given variable is small, in order to determine the values with a confidence intervals of, 95%, the t-Student distribution was applied, Spiegel (1997).

$$Rl(mm/mm) = \frac{Lt}{L'} \tag{1}$$

$$Rs = \left(\frac{4}{\pi}\right)(Rl - 1) + 1 \tag{2}$$

$$Rl(mm/mm) = \frac{St}{S_A} \tag{3}$$

3. Results

3.1 Chemical composition and "as cast" characterization

The chemical composition of the DI used is listed in Table 2.The as-cast microstructures are described in accordance with ASTMA 247 standard (Table 3). All melts were free from free carbides and the nodularity was considered suitable for this study.

Table2. Chemical composition (Wt%)

C	Si	Mn	S	P	Mg	Cu	Ni	Cr
3,32	2,36	0,31	0,012	0,016	0,033	0,62	0,025	0,058

Table3. Characterizationof the as-cast condition (ASTM A247).

Nodule count [nod/mm^2]	Nodularity	Nodule size
100	>95%	6

3.2 Heat treatments

The resultant microstructures from the different heat treatment cycles are shown in Fig.3. The Brinell hardness values from each microstructure are listed in Table 4. The results are in agreement with the specific literature, Ductile Iron Data for Design Engineers (1990).

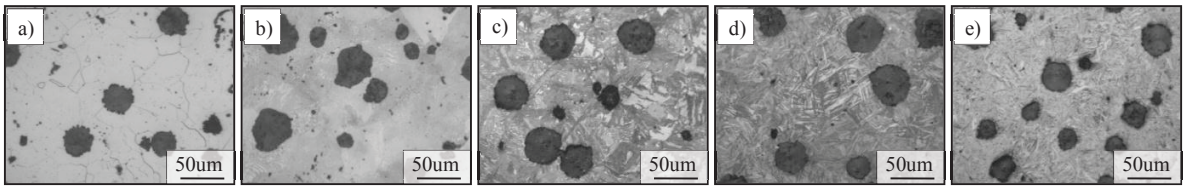

Fig.3. Microstructures.(a) Ferritic; (b) Pearlitic (as cast); (c) ADI360; (d)ADI280; (e) Martensitic

Table 4. Hardness values in each microstructure

Microstructure	F	P	ADI_{360}	ADI_{280}	M
Brinell Hardness	149	272	350	456	580

3.3. Fracture profiles

The Rs values for each fracture profile are shown in Fig. 4. The results show that for the lower toughness DI grades, such as pearlitic and martensitic, the roughness suffers no significant change as a function of the loading conditions. This is verified by the similarity observed on the fracture surfaces under the SEM (Fig.5). On the other hand, slight but consistent changes in Rs are observed as plastic deformation becomes more important in the predominant failure mechanisms, as for high temperature impact and bending tests, on ferritic and ADI microstructures. This effect is more evident in the fracture profiles of ferritic matrixes (Fig.6).For this microstructure, several authors report that the predominant fracture mechanism tends to change from fragile to ductile as the temperature increases. A marked influence of the load application rate is also reported. The nucleation, growth and coalescence of microvoids, together with the deformation of the nodular cavities, tend to be the principal feature governing the fracture mechanisms when quasistatic loads at room temperature are applied as is reported by Martinez (2010) and Fernandino et.al. (2012).

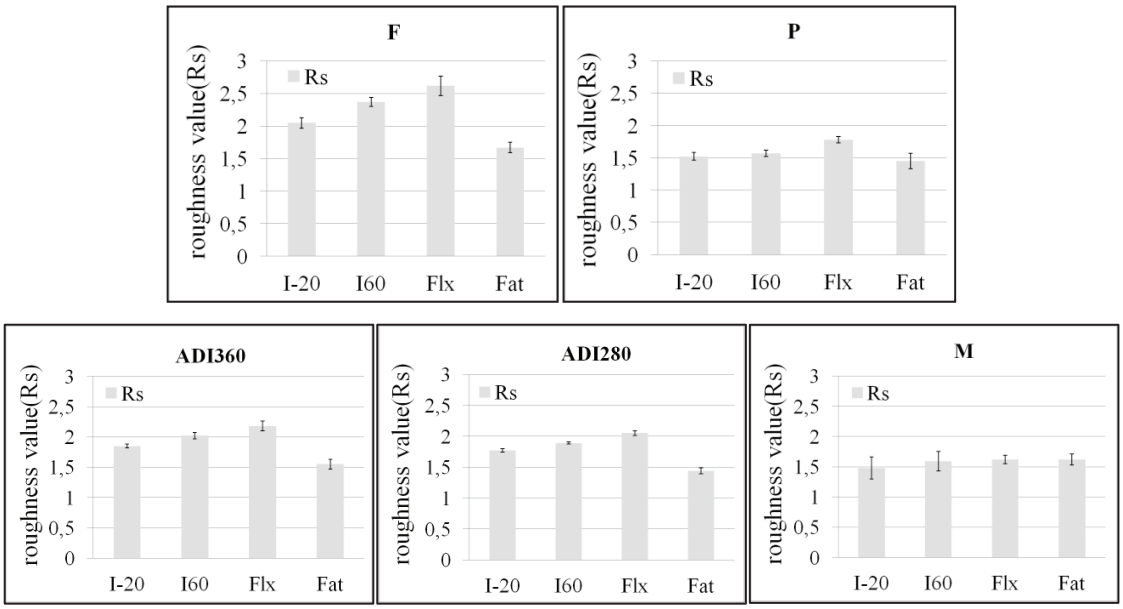

Fig.4. Rs value from the fracture profiles.

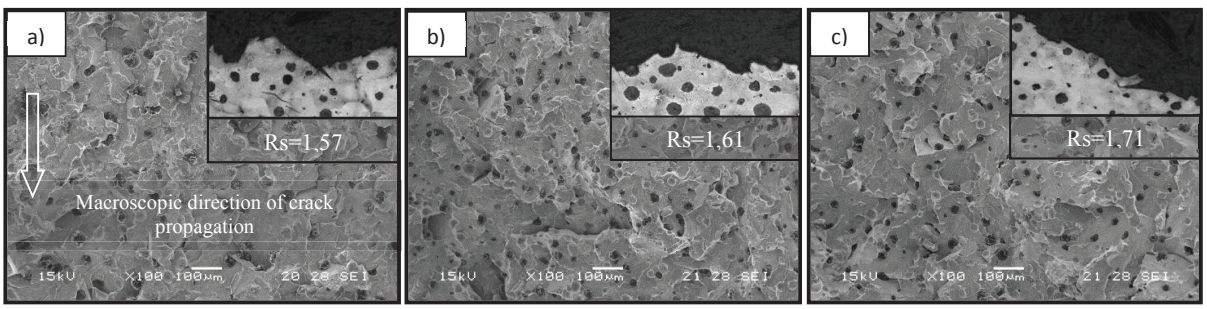

Fig.5. Fracture surfaces and profiles from impact and bending tests. Arrows indicate the direction of macroscopic crack propagation (a) PI-20; (b) PI60; (c) Pflx.

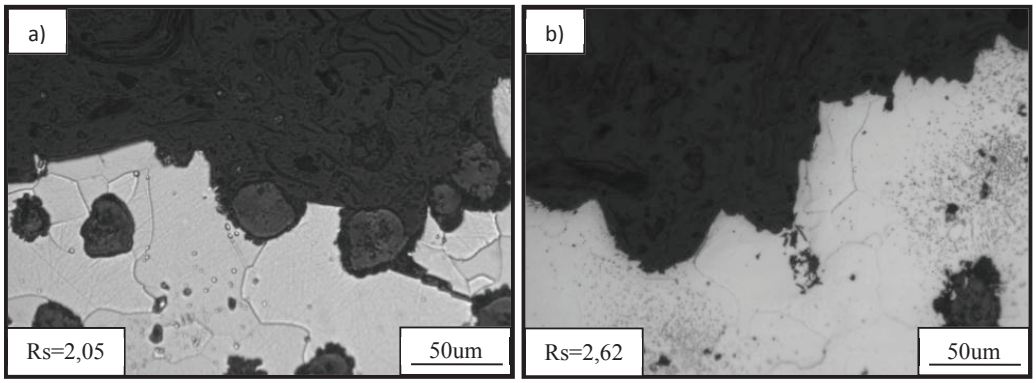

Fig.6. Fracture profiles. FDI; (a) FI-20, (b) Fflx.

For fatigue fracture of ferritic and ADI microstructures, Rs values are significantly lower than those measured for other loading conditions. The characteristics of cyclic loading in such microstructures lead to lower surface roughness and in consequence, the fracture surfaces have a “flatter" topography. Such remarkable changes in the fracture surface topography were clearly distinguishable in both SEM fractographies and optical fracture profiles. The fracture surfaces from bending and fatigue test on ADI_{360} are shown in Fig.7. The topographic change of the fracture surface and its corresponding profile is evident, clearly corresponding with the Rs value measured for each condition.

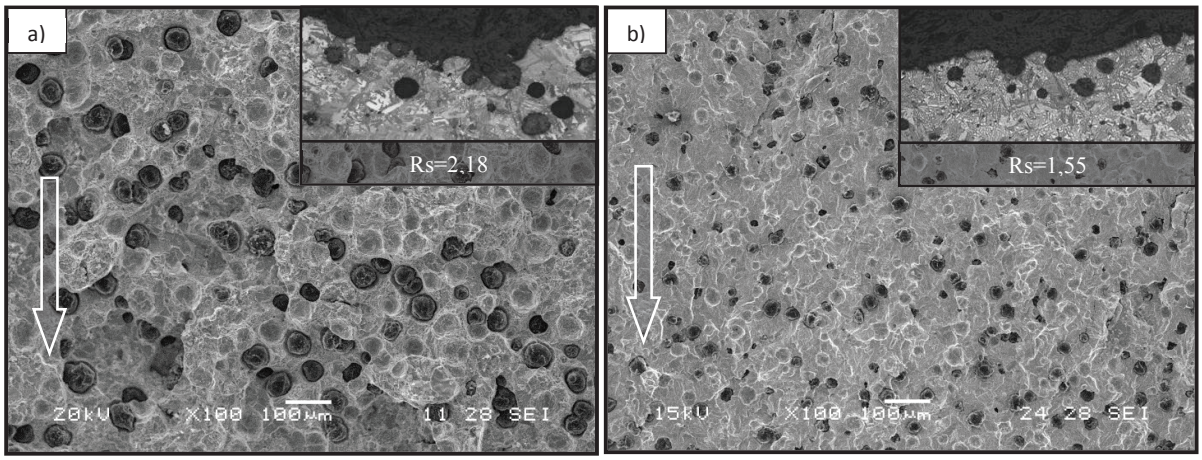

Fig. 7. Fracture surfaces and profiles from bending and fatigue tests. Arrows indicate the direction of macroscopic crack propagation (a)ADI_{360}flx; (b) ADI_{360}Fat

In the case of pearlitic and martensitic microstructures, no differences were found in the fractographic features after applying different loading conditions, possibly due to the fact that the predominant fracture mechanism does not change significantly. These trends in the Rs values are consistent with those reported by Bermont et.al (2002) for similar test conditions.

The results of the measurement of Ry are shown in Fig.8. For ferritic and ADI matrixes, as ductile fracture mechanisms became more preponderant, the Ry value increases in concordance with Rs values reported. However, a clear difference between the tree loading conditions was observed for the pearlitic matrix. The fracture profile resulting from bending test showed Ry values of 178 µm approximately,whereas, in the fatigue test, Ry was close to 82µm. The opposite trend was found in the martensitic matrix, where the highest Ry values were obtained for the bending test (approximately 100 µm). In this case, the Ry value resultant from the impact test was significantly

lower (about 57 μm). These differences can be related to the nature of the failure mode. For pearlitic ductile iron, quasi-cleavage was the predominant fracture mechanisms when impact and bending tests were performed. In fatigue test, the cyclic loads produce a fracture surface mixed between quasi-cleavage and ductile striation zones, which markedly decrease the Ry value.

For the fatigue tests on martensitic ductile iron, a rapid propagation of the crack at low cycles, with a relatively short stage of stable propagation and arrest of crack was observed. Different proportions of cleavage areas (predominantly in the stable propagation phase) and intergranular fracture were the main fracture mechanisms observed. The fracture surface resulting from impact and bending tests on martensitic ductile iron are shown in Fig.9. For the slow loading rate, the intergranular fracture mechanisms began to have a major prevalence and in consequence, a marked increase of Ry values related to the values reported for impact and bending fracture profiles, where the quasi-cleavage prevailed on the intergranular fracture.

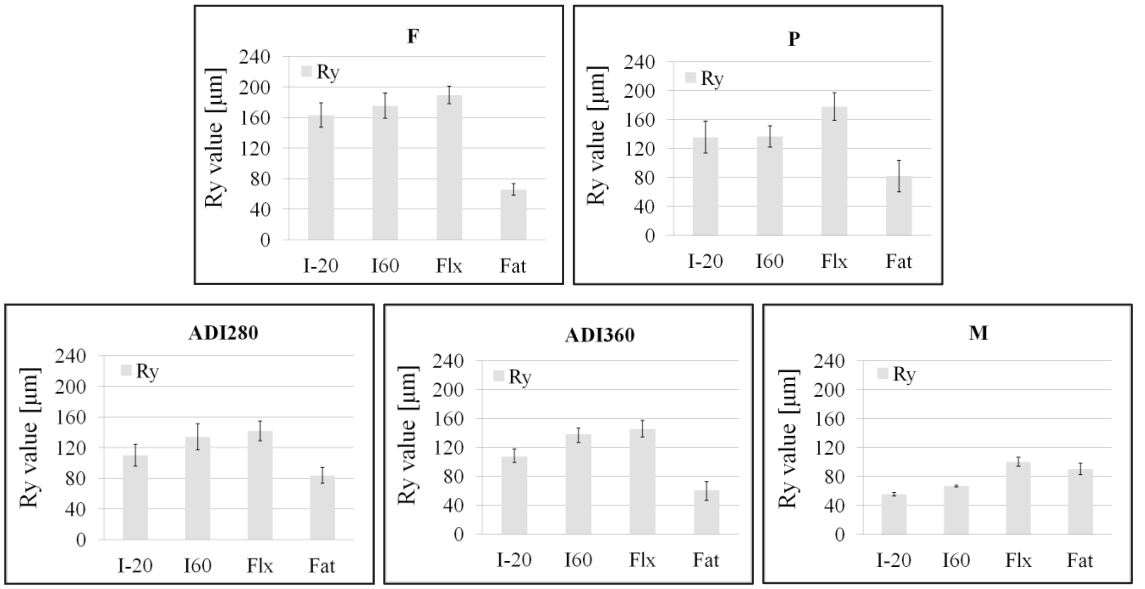

Fig.8. Ry values measured from the fracture profiles on martensitic ductile iron

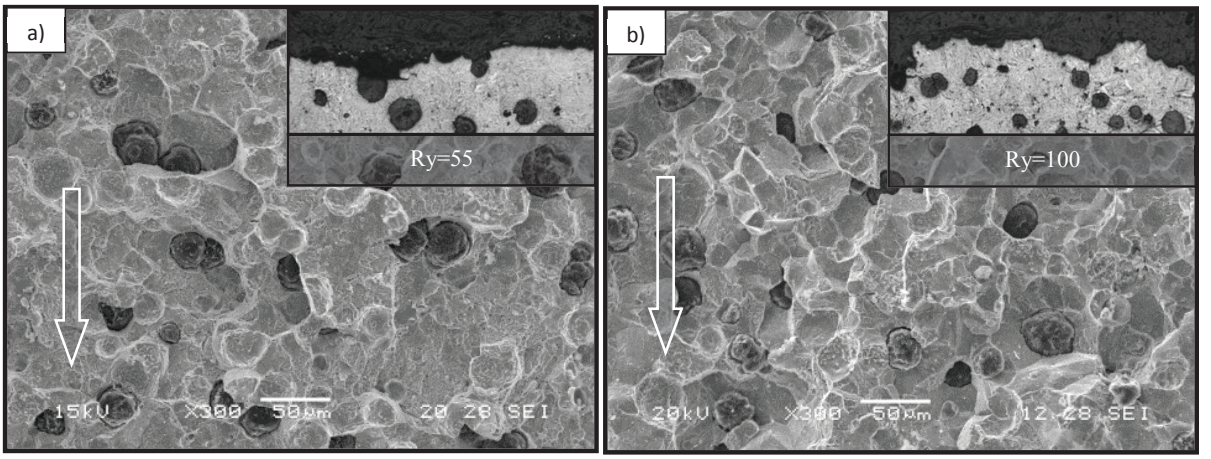

Fig. 9. Fracture surfaces and profiles from impact and bending tests. Arrows indicate the direction of macroscopic crack propagation MDI (a)MI-20; (b) Mflx.

Representative micrographs of the fracture profiles of the impact (-20ºC; 60ºC), bending and fatigue test are shown in Fig.10.

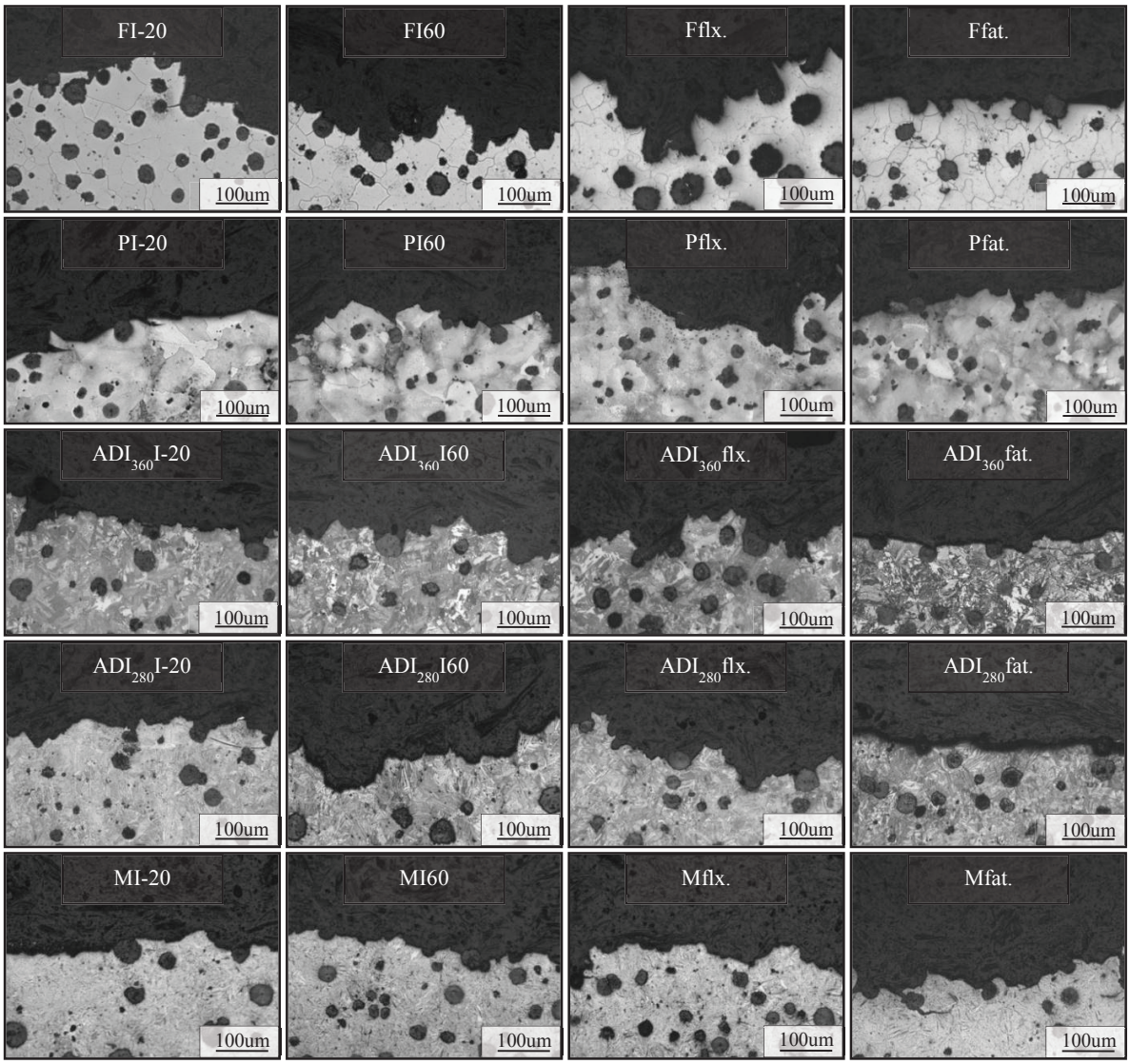

Fig.10. Fracture profile from different test conditions.

4. Conclusions

The results show that the Rs and Ry values measured on the fracture profiles show variations depending of the ductile iron microstructure and the kind of load applied.

For the lower toughness DI grades, such as those showing pearlitic and martensitic matrices, the Rs roughness parameter suffers no significant change as a function of the loading conditions. On the other hand, noticeable differences of the values of the Ry parameter were observed between the tree loading conditions.

For the higher toughness DI grades, such as those showing ferritic and ausferritic matrices, slight but consistent changes in Rs and Ry are observed as plastic deformation becomes more important in the predominant failure

mechanisms. For fatigue fracture, the values are significantly lower than those measured for other loading conditions.

The results of this study suggest that the measurements of the roughness parameters on the fracture surfaces of unknown origin can be potentially useful to identify the fracture processes and to add information to the classic fractographic analysis. Nevertheless, before values of Rs and Ry can be applied reliably to state failure modes, it is necessary to carry out extensive studies, accounting for the influence of variables not considered in the present study, such as nodule count and nodularity.

Acknowledgements

The authors are grateful to CONICET and the National University of Mar del Plata for their financial support and to MEGAFUND S.A. for providing the ductile iron used in this study.

References

Di Cocco,V.,Iacoviello,F.,Cavallini,M.,2010.Damaging micromechanisms characterization of a ferritic ductile cast iron.Engineering fracture Mechanics 77, 2016-2023.

Fernandino,D., Boeri,R.,2012. Análisis de las superficies de fractura generadas por impacto y flexión, en probetas de fundición gris esferoidal ferrítica. Proceedings CONAMET/SAM, 2012,Octubre, Viña del Mar,Chile.

Rajnovic,D., Eric,O., Sidjanin,L.,2008. Transition temperature and fracture mode of as-cast and austempered ductile iron. Journal of Microscopy232 605–610.

Ductile Iron Data for Design Engineers (1990).Cap. XII Specifications.

Eldoky,L., Voigt,R.C.,1986.Fracture of Ferritic Ductile Cast Iron. Transactions of the American Foundrymen's Society94. Minneapolis, Minnesota; USA; May 1986. 621-630.

Underwood,E., Banerji,K.,1987. Metal Handbook, 9th ed., Vol. 12, ASM, Metals Park, OH, 193-211.

Iacoviello,F.,DiBartolomeo,O., DiCocco,V.,Piacente,V.,2008. Damaging micromechanisms in ferritic-perlitic ductile cast irons. Materials science and Engineering A 478, 181-186.

Greno,G.L., Otegui,J.L.,Boeri,R.E.,1999.Mechanism of fatigue crack growth in Austempered Ductile Iron. Int. J. of fatigue 21, 35-43.

Ortiz,J.E., Cisilino,A.P., Otegui,J.L.,2001.Boundary element analysis of fatigue crack propagation micromechanisms in austempered ductile iron. Engineering Analysis with Boundary Elements 25 467-473.

Liu,J.L., Hao,X.Y.,Li,G.L.,Liu.G.Sh., 2002. Microvoid evaluation of ferrite ductile iron Ander strain. Materials letters 56 748-755.

Jen,K., Wu,J., Kim,S.,1992. Study of Fracture and Fatigue Behavior of Austempered Ductile iron. AFS Transactions100, 833-846.

Masud, L., Martínez,R., Simison,S.,Boeri,R.,2003.Embrittlement of austempered ductile iron on contact with water - Testing under applied potential. Journal of Materials Science 38, Issue 13,2971-2977.

Cavallini,M.,Bartolomeo,O.,Iacoviello,F.,2008.Fatigue crack propagation damaging micromechanisms in ductile cast iron. Engineering Fracture Mechanics 75 694-704.

Chapetti, M.D.,Cianci,S.,Boeri,R.,2000 Limite de fatiga en fundiciones nodulares austemperizadas (ADI). Proceedings SAM 513-517.

Hafiz,M.F., Hammouda,A., El-Gemae.S., 2005.Impact Properties and Fractography of Spheroidal Graphite Cast Irons.AFS Transactions 2005 American Foundry Society, Schaumburg, II. USA 2-12.

M.R.Spiegel. Estadística, Segunda Edición 1997, Schaum, Mc Graw Hill.

Bonora,N.,Ruggiero,A., 2005.Micromechanical modeling of ductile cast iron incorporating damage. Part I.Ferritic ductile cast iron. International Journal of Solids and Structures 42, 1401-1424.

Dai,P.Q.,He,Z.R., Zheng,C.M., Mao,Z.Y., 2001.In situ SEM observation on the fracture of austempered ductile iron. Materials Science and Engineering A 319,531-534.

Martinez,R.A., 2010. Fracture surfaces and the associated failure mechanisms in ductile iron with different matrices and load bearing. Engineering Fracture Mechanics 77, 2749–2762.

Voigt, R.C.,Eldoky,L.M.,1986. Crack Initiation and Propagation in As-Cast and Fully Pearlitic Ductile Cast Irons. Transactions of the American Foundrymen's Society 94, Minneapolis, Minnesota,USA, 637-644.

S. Shibutani, S. Komatsu, Y.Tanaka. Embrittlement of austempered spheroidal graphite cast iron by contact with water and resulting preventive method. International Journal of CastMetalsResearch Vol. 11, Issue 6, (1999), 579-585.

Bermont,V.M.,Castillo,R.N.,Sikora,R.N.,2002.Fracture surfaces and Mechanical properties in Ductile Iron. ISIJ International42, Nº 11,1303-1308.

Voigt, C.R.,Lee,H.Y.,Tu,Chen-Hui.,1991. Use of hardenability data to determine alloy requeriments for austempered ductile iron. Proccedings of the 1991 World ADI conference, March,Chicago,Il, 479-515.